water

MDPI

Article

Co-Pyrolysis of Fenton Sludge and Pomelo Peel for Heavy Metal Stabilization: Speciation Mechanism and Risk Evaluation

Cheng Huang [1,2,3], Lixian Wang [1], Lingyi Fan [3] and Yong Chen [1,*]

[1] School of Environmental and Engineering, Huazhong University of Science and Technology, Wuhan 430074, China; chenghuang@just.edu.cn (C.H.)
[2] Jiangxi Jindalai Environmental Protection Co., Ltd., Nanchang 330100, China
[3] School of Environmental and Chemical Engineering, Jiangsu University of Science and Technology, Zhenjiang 212003, China
* Correspondence: ychen@mail.hust.edu.cn; Tel./Fax: +86-511-84400076

Abstract: The safe disposal and resource utilization of Fenton sludge (FS) are challenges due to the presence of heavy metals (HMs). Co-pyrolysis with biomass waste can effectively increase biochar quality and immobilize HMs, but research focusing on heavy metal stabilization from Fenton sludge using the co-pyrolysis approach is scattered. In this study, the co-pyrolysis of FS and pomelo peel (PP) was developed as a strategy to reduce the environmental risk of HMs. The results showed that co-pyrolysis greatly increased the pH and aromaticity of biochars, and the maximum specific surface area was 6.5 times higher than the corresponding FS-based biochar due to the sponge-like structure of PP, which was likely conducive to adsorbing HMs during pyrolysis. Meanwhile, the addition of PP promoted the enrichment of HMs in co-pyrolyzed biochars as well as induced the transformation of bio-available HM fractions to stable forms, especially at high temperatures. Finally, the presence of PP led to the decline in HM leachability in biochars; thus, the potential ecological risks of HMs decreased from considerable pollution levels to moderate and even clean levels. This study demonstrated that co-pyrolysis with PP is a promising approach to reduce the toxicity of HMs and improve the functionality of biochar for industrial sludge management.

Keywords: Fenton sludge; co-pyrolysis; biochar; heavy metals; ecological risk

check for updates

Citation: Huang, C.; Wang, L.; Fan, L.; Chen, Y. Co-Pyrolysis of Fenton Sludge and Pomelo Peel for Heavy Metal Stabilization: Speciation Mechanism and Risk Evaluation. *Water* **2023**, *15*, 3733. https://doi.org/10.3390/w15213733

Academic Editors: Laura Bulgariu, Guoshuai Liu and Minhua Cui

Received: 19 September 2023
Revised: 12 October 2023
Accepted: 19 October 2023
Published: 26 October 2023

Copyright: © 2023 by the authors. Licensee MDPI, Basel, Switzerland. This article is an open access article distributed under the terms and conditions of the Creative Commons Attribution (CC BY) license (https://creativecommons.org/licenses/by/4.0/).

1. Introduction

The Fenton oxidation process has been widely applied in industrial wastewater treatment for the efficient degradation of refractory organics [1]. However, a large amount of Fenton sludge (FS) is inevitably produced from the neutralization step of acidic effluent, which contains high contents of ferric iron, organic contaminants, sediment impurities, and heavy metals (HMs). Among the above-mentioned contaminants, HMs (Pb, Zn, Cu, Cr, etc.) pose a significant threat to ecosystems and humans due to their non-biodegradability and strong biological toxicity [2]. Therefore, it is necessary to develop a proper sludge management strategy to eliminate or alleviate potential environmental pollution caused via HMs in FS.

In the past decade, pyrolysis has been proven as an alternative technology for sludge disposal, in which a reduction in sludge volume, heavy metal passivation, and resource recovery (e.g., biofuels and biochar) can be achieved simultaneously [3]. It has been well documented that biochar, the main product derived from the partial combustion of biomass waste, exhibits a great potential for application in pollutant removal or soil amendment [4]. Moreover, biochar is a negative carbon emission material that can facilitate achieving carbon neutrality in sludge reutilization systems. Thus, numerous researchers have focused on the optimization of pyrolysis conditions [5,6] and modification strategies of biochar [7] as well as its emerging applications [8]. However, most HMs are concentrated in the biochar matrix after pyrolysis, which may result in the potential risk of HM leaching if the sludge-derived

biochar is applied to soil and water environments. Although some studies have shown that pyrolysis contributes to the transformation of HMs from a bioavailable state into stable oxidizable and residual fractions, the immobilization of HMs largely depends on the pyrolysis temperature, species of HMs, and sludge properties. For example, a pyrolysis temperature above 600 °C is commonly necessary to improve the conversion of Mn, Cu, and Zn in sewage-sludge-based char to more stable fractions [9], while in another case, Udayanga et al. reported that Cd, Pb, and Hg in industrial sludge readily migrate at such high temperatures [10]. In addition, the characteristics of sludge (especially industrial sludge) with high ash content and low calorific value may cause more energy consumption and poor pyrolysis performance [11]. Therefore, in order to overcome these limitations, a more efficient method to immobilize HMs is urgently needed.

Recently, the co-pyrolysis of sludge with biomass waste has gained increasing attention from researchers due to its multiple benefits, including the improvement in biochar properties, the stabilization of HMs, and the reduction in energy consumption, which can be achieved simultaneously [12]. In the context of "treating the waste with the waste", various types of biomass, such as rice straw, sawdust, vegetable waste, and microalgae have been co-pyrolyzed with sludge [12–14], which has provided the potential to modify the properties of biochar as well as reduce the leaching toxicity of HMs. For instance, Dong et al. found that the co-pyrolysis of sewage sludge and rice straw exhibited great benefits for fabricating hierarchical porous structures, improving high ash content, and immobilizing heavy metals in char samples [15]. However, previous studies have mostly focused on organic-dominated sludge from municipal wastewater treatment plants; in-depth and comprehensive investigations on the co-pyrolysis of industrial sludge (such as FS) and biomass waste are still scattered. In addition, more attention should be paid to the leaching toxicity and underlying environmental risks of HMs in sludge-derived biochar.

Pomelo (*Citrus grandis*) is one of the most widely consumed fruits around the world, resulting in a large amount of pomelo peel (PP) being discarded as biomass waste. Many researchers have demonstrated that PP is a promising ingredient for the preparation of engineered carbonaceous materials due to its polymeric network structure with cellulose microfibril, hemicellulose, and lignin, which provides large specific surface areas and abundant functional groups after thermal conversion. To date, several PP-based carbon materials have been developed and applied in the adsorption of HMs, catalytic degradation and solar evaporation [16–18]. These studies inspired us to investigate whether the co-pyrolysis of FS and PP may synergistically enhance the stabilization of HMs in biochars. However, until now, the feasibility of the co-pyrolysis of pomelo peel and sludge with high concentrations of HM has not been studied.

In this study, for the first time, HMs, including Pb, Zn, Cr, and Cu, are immobilized in a biochar matrix via conducting the co-pyrolysis of pomelo peel and Fenton sludge. The main objectives of this work are to (1) explore the effect of PP addition on the characteristics of biochar and heavy metal immobilization during co-pyrolysis and (2) evaluate the single and multiple environmental risks of HMs in the biochars. This work aimed to provide a new solution to stabilize HMs in industrial sludge.

2. Materials and Methods

2.1. Feedstocks and Chemicals

Raw FS was collected from the Fenton oxidation process of an electroplating wastewater treatment plant in Wuxi, China. The fresh pomelo peel was obtained from a local fruit shop around the campus. All the feedstocks were oven dried at 105 °C for 24 h, ground finely, screened through 100 mesh and then stored in a desiccator for further use. The main properties of FS and pomelo peel are listed in Table 1.

All the chemicals used in this study, including CH_3COOH, NaOH, $NH_2OH{\cdot}HCl$, HNO_3, H_2O_2, NH_4Ac, HCl and HF were analytical grade and purchased from Shanghai Macklin Biochemical Co., Ltd., Shanghai, China.

Table 1. The main properties of FS and pomelo peel.

Parameter	FS	Pomelo Peel
pH	5.2 ± 0.1	6.9 ± 0.1
Total organic matter (TOC) (%)	4.58 ± 0.47	92.1 ± 1.05
Cu (mg/kg)	818 ± 21	ND [a]
Zn (mg/kg)	16,380 ± 231	ND
Cr (mg/kg)	128 ± 17	ND
Pb (mg/kg)	483 ± 24	ND

Note: [a] ND, Not detected.

2.2. Co-Pyrolysis of FS and PP

Co-pyrolysis experiments were conducted in a tubular furnace (OTF-1200X, Hefei Kejing Material Technology Co., Ltd., Hefei, China) as shown in Figure S1. Firstly, the pretreated FS and PP were thoroughly mixed in the agitator as the mass ratio of 1:1 based on the previous publication [19]. Then, 30.0 g of the mixed feedstock was loaded into the quartz tube and heated at different pyrolysis temperatures (300, 400, 500 and 600 °C) for 2 h. The heating rate for all the experimental groups was set invariably as 10 °C/min. During the entire pyrolysis and cooling stages, the high-pure nitrogen gas was flushed with the constant flow rate of 100 mL/min to ensure oxygen-free atmosphere. The pyrolysis products were taken out and stored after natural cooling to ambient temperature. The as-prepared samples from different temperatures were labeled as SPC300, SPC400, SPC500 and SPC600, respectively. Meanwhile, the pyrolysis of sole FS was conducted as the control test, and the procedure was same as mentioned above. The biochar samples derived from sole FS were labeled as FSC300, FSC400, FSC500 and FSC600, respectively. The specific surface area was examined using N_2 adsorption–desorption isotherm measurements equipped with an automatic specific surface analyzer (ASAP2020, Micromeritics Instruments Co., Ltd., Norcross, GA, USA). The surface functional groups of biochars were characterized using Fourier transform infrared (FTIR) spectroscopy (Nicolet iS50R, Thermo Fisher Scientific Inc., Waltham, USA). The thermogravimetric analysis was conducted using a thermogravimetric analyzer (TGA/SDTA851e MET, Shanghai Mettler Toledo Scientific Co., Ltd., Shanghai, China), following the procedure previously described [14].

2.3. Heavy Metals Analysis

2.3.1. Sequential Extraction of Heavy Metals

A modified European Communities Bureau of Reference (BCR) sequential extraction method was used to investigate the speciation of HMs in biochars, by which HMs can be classified into four fractions, namely the acid-soluble or exchangeable fraction (F1), reducible fraction (F2, bound to iron-manganese oxide), oxidizable fraction (F3, bound to organic matter and sulfide) and residual fraction (F4, primary minerals and secondary silicate lattice metals) [20]. Normally, the mobility and bio-toxicity of HMs decrease with the sequential extraction, and the order is as follows: F1 > F2 > F3 > F4. The extraction steps are provided in Table S1.

2.3.2. Leaching Experiment

The toxic characteristic leaching procedure (TCLP) recommended by the U.S. EPA was implemented to assess the leachability and ecological risk of HMs in biochar [21]. Briefly, 0.5 g of biochar was extracted by the prepared glacial acetic acid solution (pH 2.88) with the liquid-to-solid ratio of 20:1. The mixture was placed in a shaker (120 rpm) at a mesophilic temperature of 25 °C for 18 h. The extracted samples were centrifuged at 5000 rpm for 15 min, and the supernatant was filtered through a 0.22 μm PFS membrane filter prior to analysis [22].

2.3.3. Determination of Heavy Metals

The total HMs content in the samples were determined by a microwave-assisted digestion method according to the previous study [23]. Briefly, 0.200 g of sample was dissolved in the mixture of nitric acid, hydrochloric acid and hydrofluoric acid (HNO_3:HCl:HF = 6:2:1, $v/v/v$) and digested in a microwave digester (GH08Z-Z, Shanghai Metash Instruments, Shanghai, China). The detailed procedures are shown in Table S2. The total concentrations of Pb, Zn and Cr in digestion solution were determined by an inductively coupled plasma optical emission spectrometry (ICP-OES) instrument (OPTIMA 8300DV, Perkin Elmer Instrument Co., Ltd., Waltham, MA, USA).

2.4. Ecological Risk Assessment

The risk assessment code (RAC) and Nemerow pollution index (NPI) were applied to evaluate the potential environmental risk of biochar samples in this study. RAC is expressed by the proportion of F1 fraction, which represents the availability of single HM [24]. According to the RAC value, the environmental risk can be classified five levels: RAC < 1% indicates "no risk", 1% < RAC < 10% means "low risk", 10% < RAC < 30% indicated "medium risk", 30% < RAC < 50% indicates "high risk" and RAC < 50% means "medium risk".

The NPI Is one of the most widely used pollution indexes to evaluate the pollution and potential ecological risk caused by multi-contamination factors. In this study, the NPI was carried out to comprehensively assess the bioavailability and harmfulness of various heavy metals and the formula were shown as follows:

$$P_i = F_i / S_i \tag{1}$$

$$P_N = \sqrt{\left(\overline{P}_i^2 + P_{imax}^2\right)/2} \tag{2}$$

$$\overline{P}_i = \frac{\sum_{i=1}^{n} P_i}{n} \tag{3}$$

where P_i is the single pollution index of HMs in samples, F_i is the extractable concentration of HMs by the TCLP method, S_i is soil permissible limits based on the Soil Environmental Quality Standards for the developed area, in which the contents of Pb, Zn, Cr and Cu are 400, 2000, 30 and 2000 mg/kg, respectively [25]. P_N is the Nemerow integrated pollution index, P_i is the average value of the single pollution index of HMs, and P_{imax} is the maximum value of the single pollution index of HMs.

3. Results and Discussion

3.1. Properties of Sludge and Biochars

3.1.1. General Properties

The properties of biochars are strongly dependent on the elemental compositions and contents of feedstocks as well as pyrolysis conditions [26]. Thus, the properties of the feedstocks and their biochars are shown in Table 2. Both C and H contents of FS were less than 5%, indicating that the main components in the FS were inorganic elements (e.g., Fe, Zn, Cu and other HMs). On the contrary, the organic matter was the dominant component in the PP. These results were in accordance with the thermogravimetric study presented in Figure 1, in which the weight loss rate of FS reached 25%, whereas almost 80% of PP decomposed when the pyrolysis temperature increased to 600 °C.

As shown in Table 2, both the high temperature and co-pyrolysis with PP reduced the yields of biochar. For example, there was a slight decline in the biochar yield from 83.36% to 74.32% at 300 to 600 °C, indicating the high ash contents in FS. Moreover, the yields of blended biochars (47.32–71.83%) were much lower than the biochars derived from FS alone under the same pyrolysis conditions, which can be interpreted by the high organics content in PP. During pyrolysis, the main organic compounds in PP such as hemicellulose,

cellulose, lignin and aliphatic compounds readily decomposed via the demethylation, demethoxylation and decarboxylation reactions [27].

Table 2. Yield, pH and ultimate analysis of feedstocks and biochars.

Sample	Yield (%)	pH	C (%)	H (%)	H/C	SSA (m^2/g)
FS	/	5.25 ± 0.05	4.37	1.66	4.56	/
PP	/	6.95 ± 0.05	58.34	13.67	2.81	/
FSC300	83.36 ± 4.15	5.29 ± 0.08	2.29 ± 0.12	0.84 ± 0.03	4.40	2.15
FSC400	82.18 ± 3.18	5.27 ± 0.04	1.79 ± 0.18	0.63 ± 0.05	4.22	3.18
FSC500	79.46 ± 2.87	5.28 ± 0.07	1.77 ± 0.07	0.62 ± 0.08	4.20	3.74
FSC600	74.32 ± 4.43	5.80 ± 0.13	1.67 ± 0.09	0.53 ± 0.02	3.80	4.17
SPC300	71.83 ± 2.79	7.28 ± 0.06	40.67 ± 0.16	2.52 ± 0.10	0.75	18.54
SPC400	60.31 ± 4.63	8.59 ± 0.04	37.14 ± 0.14	3.07 ± 0.08	0.74	22.92
SPC500	52.43 ± 3.98	9.81 ± 0.11	34.52 ± 010	1.73 ± 0.06	0.60	27.25
SPC600	47.32 ± 3.53	10.92 ± 0.08	31.03 ± 0.08	1.14 ± 0.02	0.44	31.26

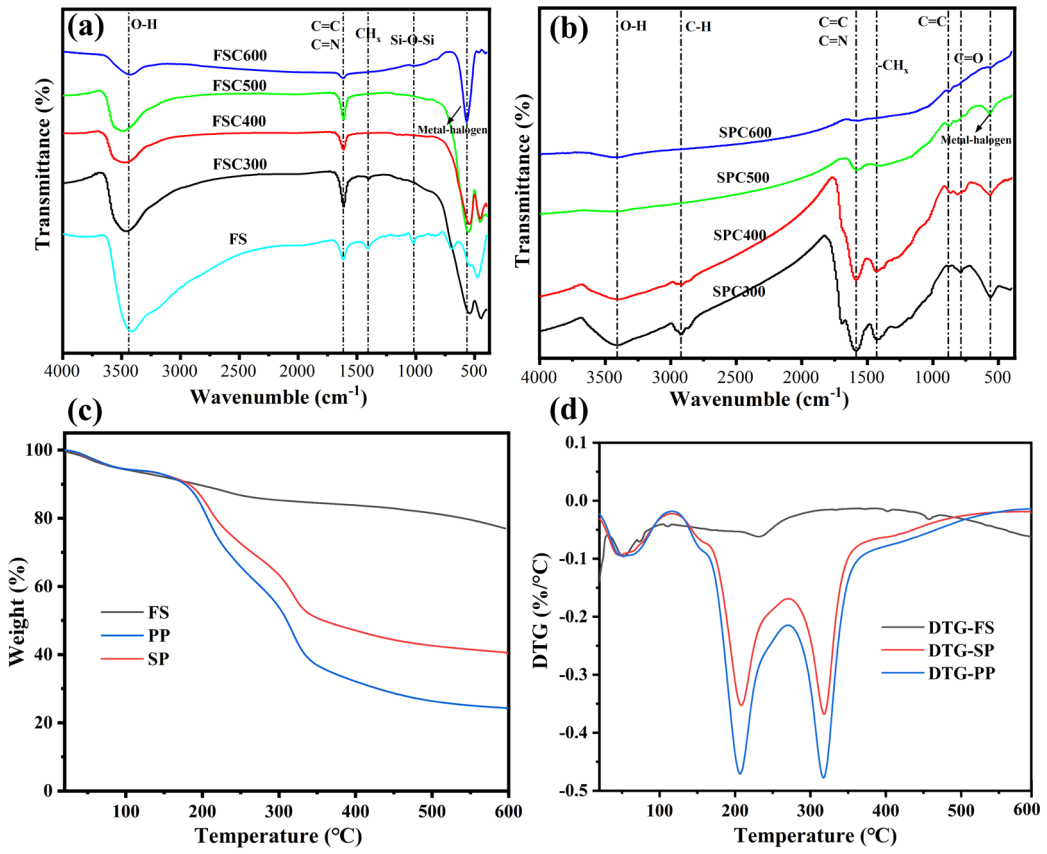

Figure 1. FTIR spectra of FS, FSC (**a**) and SPC (**b**) with different pyrolysis temperatures. TG (**c**) and DTG (**d**) curves of FS, SP and PP.

3.1.2. Elemental Analysis and Specific Surface Area

The elemental analysis of feedstocks and biochars clearly demonstrated that both C and H contents decreased with increasing pyrolysis temperature owing to the rapid decomposition of organic substances. Meanwhile, the H/C molar ratio was used to characterize the organic aromaticity degree of biochars: the H/C ratio $\leq$0.3 indicated highly condensed aromatic ring structures, whereas H/C $\geq$0.7 suggested a low condensed structures [20]. As shown in Table 2, the H/C ratios of FSC (3.80–4.40) were much higher than 0.7, showing an obvious non-condensed structure in FSC [28]. On the contrary, the molar H/C ratio of SPC decreased significantly to 0.44–0.75 with the increase in temperature, which represented

the increment of aromaticity in SPC. The pH of FSC increased slightly from 300 to 600 °C, which is attributed to the thermal decomposition of acidic functional groups and formation of alkali salts [29]. It should be noted that the pH of FS-based biochar was acidic, which is different from that of organic-dominated sludge in the previous studies [30]. One possible reason for these results is that more metal chlorides were produced during the pyrolysis of FS, contributing to the surface acidity of biochars [31]. Comparing with acidic FSC, the addition of PP resulted in a significant elevation of pH, and all the SPCs were alkaline, which is likely induced by the alkaline species such as metal carbonates and hydroxides in the PP.

Also, it could be observed that the co-pyrolysis with PP addition resulted in the increment of biochars' specific surface area (SSA). For example, the SSA of co-pyrolyzed biochar at 600 °C (31.26 m^2/g) was 6.5 times higher than that of FS-based biochar (4.17 m^2/g). This is possibly because the sponge-like structure of PP was conducive to form well-developed porous biochar during the pyrolysis process.

3.1.3. FTIR Spectra Analysis

The functional groups of FS and biochars were investigated via FTIR analysis. As shown in Figure 1a, most of the peaks, including 3435 cm^{-1} for the −OH stretching vibration, 1655 cm^{-1} for the C=C and C=N stretching vibrations in aromatic annulus and amide bonds, $-CH_x$ groups in aliphatic chains [19], weakened and even completely disappeared with the raising temperature compared with raw FS, suggesting the substantial decomposition of organic compounds. The intensity of the metal–halogen tensile vibration (approximately 570 cm^{-1}) was greatly enhanced with the increase in pyrolysis temperature, which was likely owing to the formation of metal chlorides. This is consistent with the results of acidic characteristics of FSC discussed in Section 3.1.1. After co-pyrolyzing with PP, a new peak of C=O appeared in SPC, and other functional groups were enriched compared with the corresponding peak in FSC, indicating the abundant organics in PP. This was possibly related to the ring opening, depolymerization of hemicellulose and the aromatization of benzene ring in lignin [14,32]. Moreover, the peak of metal–halogen tensile vibration decreased as the temperature rose to 600 °C, which differed from that of FSC. This could be explained by the conversions of metal halide compounds to more stable forms during the co-pyrolysis process. Similar results have also been reported in another publication [33].

3.1.4. Thermogravimetric Analysis

The thermogravimetric results of FS, PP and their mixture are shown in Figure 1c,d. The overall weight loss rates of FS, PP and SP were 23.0%, 59.8% and 76.0%, which are attributed to the higher proportion of volatile matter in PP than that of FS. For FS alone, a small weight loss peak could be observed at about 250 °C, which could be designated to the decomposition of hydrocarbons in the industrial sludge. In contrary, two strong peaks in DTG curves were presented for PP and the mixture, dividing the whole pyrolysis process into two individual stages. The first stage occurred at 180–240 °C and was due to the decomposition of pectin [34]. The second decomposition phase occurred at around 310–360 °C, which was believed to be due to the decomposition of cellulose and hemicellulose in PP [35]. The TG curve became flat after 550 °C with no obvious loss of weight for all the samples, suggesting the good thermal stability of derived biochars.

3.2. The Total Contents of HMs in the Biochars

The total contents of HMs in raw FS and biochars are presented in Table 3. The total amounts of Cu, Cr and Pb of FS were in the range of 128.55–818.68 mg/kg while the concentration of Zn was more than 16,000 mg/kg due to the dominant zinc-plating process in the electroplating factory. Most of the HMs (Pb, Zn and Cr) were enriched in the FSC, and the concentrations increased as the pyrolysis temperature rose, which is likely attributed to the thermal decomposition of organic matters and high stability of HMs [36]. However, the

contents of Cu in the FSC were found to be lower compared with that in the FS, indicating that a certain proportion of volatile Cu compounds generated and transferred to bio-oil and bio-gas. This is consistent with the previous study, in which dissatisfactory immobilization rates of Cu (33.62–67.85%) were achieved after the pyrolysis of electroplating sludge [31]. A similar change trend of HM contents could be observed in the co-pyrolyzed biochars, but the concentrations of HM in the SPC were much lower than those in the FSC, which may be attributed to the "dilution effect" caused by the HMs-free PP addition.

Table 3. Total contents and recovery rates of HMs in FS and biochar.

Sample	Pb		Zn		Cr		Cu	
	Total Content (mg/kg)	Recovery Rate (%)	Total Content (mg/kg)	Recovery Rate (%)	Total Content (mg/kg)	Recovery Rate (%)	Total Content (mg/kg)	Recovery Rate (%)
FS	483.45 ± 24.29	/	16,380 ± 231	/	128.55 ± 17.07	/	818.68 ± 21.85	/
FSC300	519.65 ±21.67	89.68 ± 3.74	17,771 ± 373	90.4 ± 1.90	145.76 ± 2.76	94.9 ± 1.80	704.25 ± 45.50	71.77 ± 4.64
FSC400	513.18 ± 26.40	87.31 ± 4.49	18,661 ± 265	93.6 ± 1.33	144.95 ± 6.83	93.06 ± 4.38	765.13 ± 20.38	76.87 ± 2.05
FSC500	530.29 ± 28.66	87.24 ± 4.71	18,939 ± 736	91.9 ± 3.57	144.63 ± 3.58	89.78 ± 2.21	796.50 ± 11.50	77.37 ± 1.12
FSC600	611.43 ± 2.76	94.08 ± 0.42	20,573 ± 891	93.3 ± 4.05	163.80 ± 3.25	95.11 ± 1.89	873.12 ± 17.63	79.33 ± 0.69
SPC300	304.64 ± 3.92	90.61 ± 1.17	10,930 ± 495	95.8 ± 4.34	94.94 ± 4.81	94.94 ± 5.40	450.63 ± 13.13	81.88 ± 2.38
SPC400	356.31 ± 16.65	88.98 ± 4.16	12,854 ± 379	94.3 ± 2.79	116.25 ± 4.25	104.25 ± 4.00	539.50 ± 35.50	79.55 ± 5.23
SPC500	469.38 ± 12.62	101.90 ± 2.74	13,121 ± 208	84.0 ± 1.33	128.94 ± 2.94	103.94 ± 1.69	677.45 ± 27.50	86.85 ± 3.53
SPC600	503.21 ± 7.69	98.60 ± 1.51	15,960 ± 603	95.7 ± 3.49	139.25 ± 0.75	99.25 ± 0.55	748.81 ± 26.19	86.64 ± 3.03

Meanwhile, the recovery rates of HMs were calculated using the following equation:

$$RR = \frac{C_B \times Y}{C_F} \times 100\% \quad (4)$$

where RR is the recovery rate of specific HM (%), C_B and C_F represent the total concentration of HMs in the feedstocks and biochars (mg/kg), and Y is the yield of biochars (%). As shown in Table 3, the RRs of Cu, Zn, Cr and Pb were 71.77–86.85%, 84.0–95.8%, 89.78–104.25% and 87.24–101.90% in FSC and SPC, respectively, indicating that most of the HMs were retained in biochars after pyrolysis. Moreover, it seems that the recovery rates of HMs in the co-pyrolytic biochars (SPC) were higher than those in the sole biochars (FSC) in most cases. For instance, the RRs of Cr in the FSC were in the range of 89.78–95.11%, while the values increased to 94.94–104.25% under co-pyrolysis with PP. These results suggested that the addition of PP was conducive to immobilizing HMs in biochar owing to the high organic carbon content of PP [37].

3.3. The Speciation of HMs in the Biochars

It is well known that the toxicity and migration characteristics of HMs in biochar largely depend on the chemical speciation. Therefore, the distribution characteristics of HM fractions in FSC and SPC were analyzed based on a modified BCR extraction procedure, and the results are shown in Figure 2. Generally, the BCR-extractable fractions of HMs can be divided into three categories: (1) both the acid-extractable (F1) and reducible (F2) fractions represent high mobility and direct toxicity, (2) the oxidizable fraction (F3) exhibits a potential toxicity due to its low degradation resistance in the certain environment, and (3) the residual fraction (F4) is non-bioavailable and extremely stable under most conditions [38]. For the raw FS, the bioavailable fractions (F1 + F2) of Pb and Zn were 49.8% and 59.7%, respectively, which indicated high ecological risks from these HMs if the FS was discharged into the aquatic and soil ecosystems. After converting FS into FSC through single pyrolysis, the bioavailable fractions (F1 and F2) of Pb were readily converted into relatively stable forms (F3 and F4) with the increasing temperature. For example, the F1 + F2 fraction of Pb decreased from 40.8% in the FSC300 to 4.42% in the FSC600, suggesting that pyrolysis in higher temperature was more beneficial to the passivation of HMs. Similar change trends were also observed in the speciation distribution of Cu and Cr. The stable fractions (F3 + F4) of Cu and Cr in FSC were more than 90% and did not change significantly

at 300–600 °C, which could be interpreted by their strong affinity to organic ligands or minerals in raw FS [19]. The F1 and F2 portions of Zn remained stable and still more than 35.1% in FSC600, while the portion of F4 increased, indicating that the transformation of oxidizable Zn complexes to more stable Zn oxide or co-crystal compounds [39].

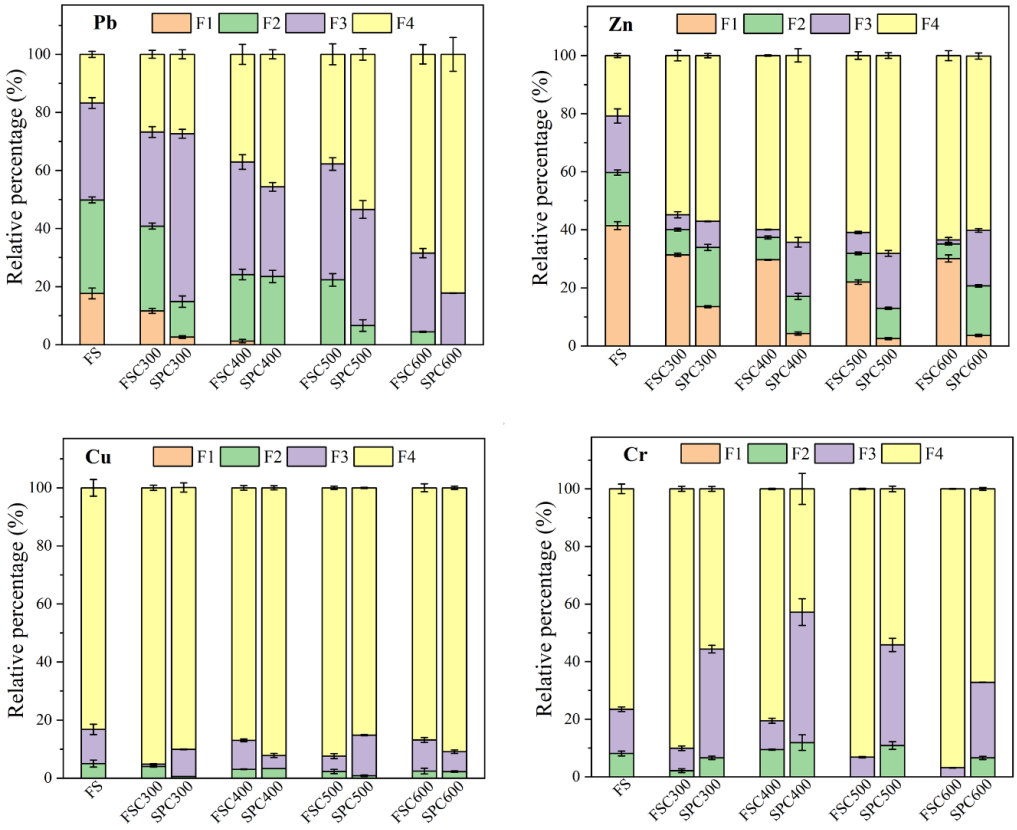

Figure 2. Speciation distribution of HMs in FS and biochars.

Co-pyrolysis with PP exhibited a remarkable effect on the distribution of HM fractions in SPC, and the change trend largely depended on the type of HMs. As to Pb, the fractions of F1 and F2 were reduced by 52.9–100% in SPC at the pyrolysis temperature of 300–600 °C, indicating that co-pyrolysis had a strong passivating effect on the Pb. Compared with the chemical speciation of Zn in FSC, the proportion of F1 and F2 in SPC declined sharply, whereas the F3 fraction increased significantly. Similar changes were observed in Cr. These results were in accordance with a previous study in which the F1, F2 and F4 fractions of all HMs decreased while the content of F3 increased with the mixture ratios of cotton stalks [40]. This phenomenon is likely attributed to the complexation reactions that occurred between the HMs and organic substance in the PP. In summary, co-pyrolysis with PP is conducive to the conversion of unstable HMs to stable species such as oxidizable and residual fractions, and it consequently decreased the bio-toxicity of HMs.

3.4. The Leaching Toxicity of HMs in the Biochars

The TCLP test was conducted to investigate the leachability of HMs in the biochars, and the results are presented in Figure 3. The limit values of HMs were 100 mg/L for Zn and Cu, 15 mg/L for Cr and 5 mg/L for Pb based on the identification standards for hazardous wastes in China [6]. The leachable contents of Cr, Pb and Cu in raw FS did not exceed the threshold values, while the contents of Zn in the TCLP leachate was 642.08 mg/L, which was 5.42 times higher than that of permissible limits, indicating the potential risk of Zn pollution to the environments. After converting FS to FSC, the leaching of HMs was significantly suppressed ($p < 0.05$) and continuously fell off with the rising temperature. For instance, the leached concentrations of Zn, Cr, Cu and Pb in FSC600

exhibited the remarkable declines of 61.4%, 46.0%, 92.8% and 100%, respectively, compared with those in raw FS. These results agreed with the change trend of chemical speciation of HMs and could be attributed to the formation of more stable structures (e.g., metal–silicate and metal–oxide) in the carbon matrix [19].

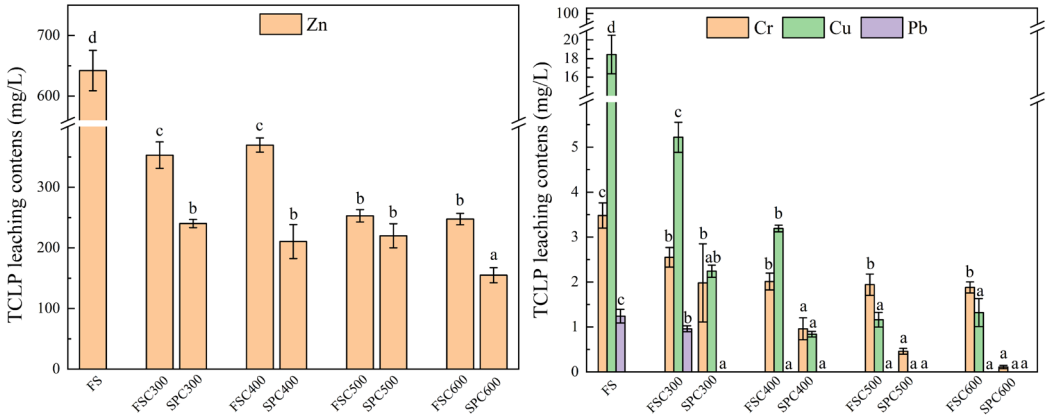

Figure 3. The TCLP leaching contents of HMs in FS and biochars. The lowercase letters above the bars show significant differences of each bar of data ($p < 0.05$, n = 3).

As for the SPC, the toxic leachability of HMs was further decreased after the co-pyrolysis process. Although the leachable content of Zn in SPC remained higher than the limit value, the addition of PP notably decreased the leaching content of Zn from 6.42-fold of threshold values to less than 2.5 times in the temperature range. In addition, no leachable Cu and Pb were detected in SPC500 and SPC600, indicating that the co-pyrolysis of sludge and PP effectively enhanced the immobilization of HMs and reduced the toxic leaching of them to environments. There are some possible reasons for the results: (i) the generation of a more stable structure such as organometallic compounds and metal–oxide in the carbon matrix is stimulated by the presence of PP [39], and (ii) the well-developed pores and abundant functional groups of SPC are capable of trapping or absorbing the metal(loid)s [41]. Furthermore, several mechanisms including a carbon shield, complexation interactions and electrostatic interactions were likely involved in the immobilization of HMs [21]; further study is needed to comprehensively reveal the contribution of the main ingredients in PP during pyrolysis.

3.5. The Environmental Risk Evaluation of HMs in the Biochars

The ecological risks of single and multiple HMs in biochars were evaluated using several indicators including a risk assessment code (RAC) and Nemerow pollution index (NPI). As shown in Figure 4, the risk levels for Pb (17.6) and Zn (41.4) in FS were considered as medium and high pollution levels, respectively (Cr and Cu were not listed due to there being no detectable F1 form in this study). After pyrolysis, the pollution level of Pb in FSC reduced to low risk level (1.2) at 400 °C and further reduced to a clean level at 500–600 °C, while the RAC values of Zn declined by 27.2–46.9% with the increasing temperature, indicating a high or moderate pollution risk for FSC. These results suggested that pyrolysis could improve the transformation of the F1 fraction of HMs to other stable forms, but the passivation was not very satisfactory for Zn. In contrary, co-pyrolysis with PP could further decrease the risk level of HMs in biochars. The RACs of Pb in SPC were significantly decreased to 2.6 at 300 °C, and even Pb is not detected at 400–600 °C, presenting low-risk or no-risk levels in the co-pyrolytic biochars. Apart from SPC300, other SPC samples exhibited a low environmental risk level for Zn, indicating the positive effect of co-pyrolysis on the Zn immobilization.

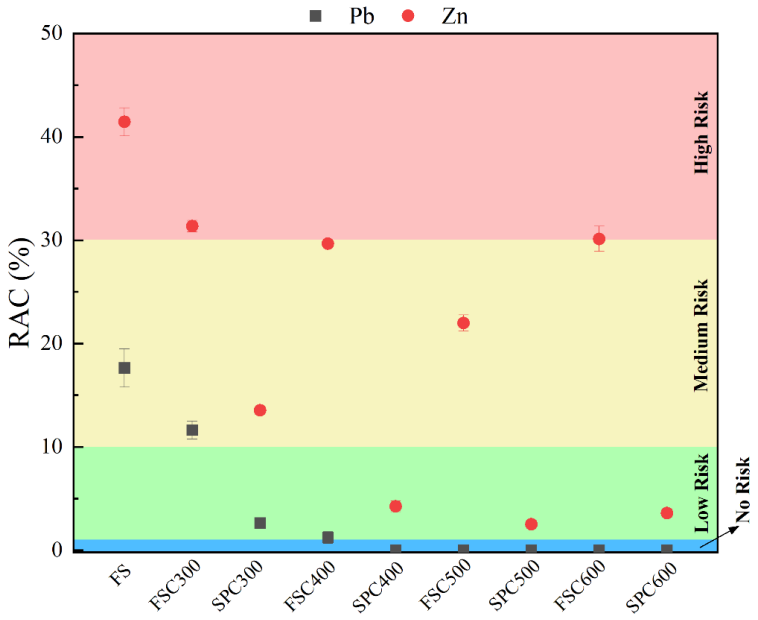

Figure 4. The potential ecological risk (RAC) of Pb and Zn in biochars.

The results of NPI assessment and the classification level of the HMs pollution are presented in Table 4. The P_N value of FS was 9.62, which far exceeded the threshold of the "serious" pollution level. This indicated that it posed an extremely high contamination risk if FS was directly applied into soil. The P_N values of FSC decreased from 9.62 to 5.33, 3.64, 5.53, and 3.13 for FSC300–600, respectively, which were considered at a "severe" risk level. Furthermore, co-pyrolytic biochars showed more positive impacts in decreasing the NPI: especially the comprehensive pollution level of SPC600 was the lowest, belonging to a "moderate" pollution degree. These results suggested that co-pyrolysis with PP is a promising strategy to reduce the ecological risk of HMs in industrial sludge. However, both the RAC and NPI values of co-pyrolyzed biochars were higher than the expected results due to the high contents of HMs in FS, and thereby, further study is still required for a comprehensively technical optimization and potential application prospects of biochar in pilot-scale trials.

Table 4. The Nemerow pollution index (P_i/P_N) of HMs in FS and biochars.

Sample	P_i				P_N	Classification Level
	Pb	Zn	Cr	Cu		
FS	12.84	4.64	0.37	0.12	9.62	Serious
FSC300	7.06	3.40	0.10	0.10	5.33	Severe
FSC400	4.80	2.64	0.04	0	3.64	Severe
FSC500	7.39	2.68	0.06	0	5.53	Severe
FSC600	4.21	1.28	0.02	0	3.13	Severe
SPC300	5.06	2.59	0.02	0	3.82	Severe
SPC400	4.40	0.61	0	0	3.23	Severe
SPC500	4.95	2.51	0.03	0	3.74	Severe
SPC600	3.10	0.15	0	0	2.26	Moderate
Pollution degree	$P_i/P_N < 1$, low contamination; $1 < P_i/P_N < 3$, moderate contamination; $3 < P_i/P_N < 6$, severe contamination; $P_i/P_N > 6$, serious contamination.					

4. Conclusions and Future Perspectives

In this study, the effect of co-pyrolysis of FS and PP on the stabilization of HMs was firstly investigated. The addition of PP decreased the yield rate but improved the properties of co-pyrolytic biochar including pH, aromaticity, specific surface area and functional groups. Furthermore, co-pyrolysis with PP could reduce the total contents of HMs (i.e., Pb,

Zn, Cr and Cu) in biochar, and the transformation from bio-available (F1 + F2) to stable fractions (F3 + F4) was achieved simultaneously. The TCLP leaching test demonstrated that the leachable concentrations of HMs in co-pyrolyzed biochar were greatly decreased, thereby reducing the potential ecological risks of single (RAC) and multiple (NPI) HMs from "high" to "moderate" and even "low" risk degrees. Therefore, co-pyrolysis with PP was considered as a feasible strategy to immobilize HMs in industrial sludge. However, the immobilization performance of HMs in FS should be further improved via technical parameter optimization and other carbonization technologies application due to high HM contents in industrial sludge. In addition, the co-pyrolysis of PP and different type of industrial sludge in the long-term application should be comprehensively evaluated before its practical application to soil.

Supplementary Materials: The following supporting information can be downloaded at: https://www.mdpi.com/article/10.3390/w15213733/s1, Figure S1: Fixed bed reactor system for co-pyrolysis; Table S1: Details of BCR extraction procedure and extraction fluids; Table S2: Microwave digestion procedure used in this study.

Author Contributions: Conceptualization, Y.C. and C.H.; methodology, L.W. and L.F.; validation, C.H., L.W. and L.F.; data curation, L.W.; writing—original draft preparation, C.H.; writing—review and editing, C.H.; visualization, C.H.; supervision, Y.C.; project administration, Y.C.; funding acquisition, C.H. All authors have read and agreed to the published version of the manuscript.

Funding: This study was funded by the Natural Science Foundation of Jiangsu Province (Grant No. BK20201001), the Postdoctoral Science Foundation of China (Grant No. 2021M701512), the Post-doctoral Preferred Funding Project of Jiangxi (Grant No. 2020KY36) and the Open Research Fund of Changjiang Survey Planning Design and Research Co., Ltd. (CX2020K09).

Institutional Review Board Statement: Not applicable.

Informed Consent Statement: Not applicable.

Data Availability Statement: Not applicable.

Conflicts of Interest: The authors declare no conflict of interest.

References

1. Gao, L.; Cao, Y.; Wang, L.; Li, S. A review on sustainable reuse applications of Fenton sludge during wastewater treatment. *Front. Environ. Sci. Eng.* **2021**, *16*, 77. [CrossRef]
2. Yaqoob, A.A.; Ahmad, H.; Parveen, T.; Ahmad, A.; Oves, M.; Ismail, I.M.I.; Qari, H.A.; Umar, K.; Mohamad Ibrahim, M.N. Recent Advances in Metal Decorated Nanomaterials and Their Various Biological Applications: A Review. *Front. Chem.* **2020**, *8*, 341. [CrossRef] [PubMed]
3. Chai, Y.; Huang, C.; Sui, M.; Yin, Y.; Sun, N.; Chen, Y.; Liao, Z.; Sun, X.; Shen, W.; Tang, S. Fe-loaded alginate hydrogel beads activating peroxymonosulfate for enhancing anaerobic fermentation of waste activated sludge: Performance and potential mechanism. *J. Environ. Manag.* **2023**, *341*, 118079. [CrossRef]
4. He, M.; Xu, Z.; Hou, D.; Gao, B.; Cao, X.; Ok, Y.S.; Rinklebe, J.; Bolan, N.S.; Tsang, D.C.W. Waste-derived biochar for water pollution control and sustainable development. *Nat. Rev. Earth Environ.* **2022**, *3*, 444–460. [CrossRef]
5. Hossain, M.K.; Strezov, V.; Chan, K.Y.; Ziolkowski, A.; Nelson, P.F. Influence of pyrolysis temperature on production and nutrient properties of wastewater sludge biochar. *J. Environ. Manag.* **2011**, *92*, 223–228. [CrossRef] [PubMed]
6. Jin, J.; Li, Y.; Zhang, J.; Wu, S.; Cao, Y.; Liang, P.; Zhang, J.; Wong, M.H.; Wang, M.; Shan, S.; et al. Influence of pyrolysis tem-perature on properties and environmental safety of heavy metals in biochars derived from municipal sewage sludge. *J. Hazard. Mater.* **2016**, *320*, 417–426. [CrossRef]
7. Zhang, J.; Shao, J.; Jin, Q.; Li, Z.; Zhang, X.; Chen, Y.; Zhang, S.; Chen, H. Sludge-based biochar activation to enhance Pb(II) adsorption. *Fuel* **2019**, *252*, 101–108. [CrossRef]
8. Mian, M.M.; Alam, N.; Ahommed, M.S.; He, Z.; Ni, Y. Emerging applications of sludge biochar-based catalysts for environ-mental remediation and energy storage: A review. *J. Clean. Prod.* **2022**, *360*, 132131. [CrossRef]
9. Li, D.; Shan, R.; Jiang, L.; Gu, J.; Zhang, Y.; Yuan, H.; Chen, Y. A review on the migration and transformation of heavy metals in the process of sludge pyrolysis. *Resour. Conserv. Recy.* **2022**, *185*, 106452. [CrossRef]
10. Udayanga, W.D.C.; Veksha, A.; Giannis, A.; Liang, Y.N.; Lisak, G.; Hu, X.; Lim, T.-T. Insights into the speciation of heavy metals during pyrolysis of industrial sludge. *Sci. Total Environ.* **2019**, *691*, 232–242.
11. Feng, S.; Zhang, G.; Yuan, D.; Li, Y.; Zhou, Y.; Lin, F. Co-pyrolysis of paper mill sludge and textile dyeing sludge with high calorific value solid waste: Pyrolysis kinetics, products distribution, and pollutants transformation. *Fuel* **2022**, *329*, 125433. [CrossRef]

12. Ma, M.; Xu, D.; Zhi, Y.; Yang, W.; Duan, P.; Wu, Z. Co-pyrolysis re-use of sludge and biomass waste: Development, kinetics, synergistic mechanism and industrialization. *J. Anal. Appl. Pyrol.* **2022**, *168*, 105746. [CrossRef]
13. Li, Y.; Yu, H.; Liu, L.; Yu, H. Application of co-pyrolysis biochar for the adsorption and immobilization of heavy metals in contaminated environmental substrates. *J. Hazard. Mater.* **2021**, *420*, 126655. [CrossRef] [PubMed]
14. Peng, B.; Liu, Q.; Li, X.; Zhou, Z.; Wu, C.; Zhang, H. Co-pyrolysis of industrial sludge and rice straw: Synergistic effects of biomass on reaction characteristics, biochar properties and heavy metals solidification. *Fuel Process. Technol.* **2022**, *230*, 107211. [CrossRef]
15. Dong, Q.; Zhang, S.; Wu, B.; Pi, M.; Xiong, Y.; Zhang, H. Co-pyrolysis of Sewage Sludge and Rice Straw: Thermal Behavior and Char Characteristic Evaluations. *Energy Fuels* **2020**, *34*, 607–615. [CrossRef]
16. Lu, J.; Kumar Mishra, P.; Hunter, T.N.; Yang, F.; Lu, Z.; Harbottle, D.; Xu, Z. Functionalization of mesoporous carbons de-rived from pomelo peel as capacitive electrodes for preferential removal/recovery of copper and lead from contaminated water. *Chem. Eng. J.* **2022**, *433*, 134508. [CrossRef]
17. Wang, W.; Chen, M. Catalytic degradation of sulfamethoxazole by peroxymonosulfate activation system composed of nitrogen-doped biochar from pomelo peel: Important roles of defects and nitrogen, and detoxification of intermediates. *J. Colloid Interf. Sci.* **2022**, *613*, 57–70. [CrossRef]
18. Geng, Y.; Sun, W.; Ying, P.; Zheng, Y.; Ding, J.; Sun, K.; Li, L.; Li, M. Bioinspired Fractal Design of Waste Biomass-Derived Solar–Thermal Materials for Highly Efficient Solar Evaporation. *Adv. Funct. Mater.* **2021**, *31*, 2007648. [CrossRef]
19. Wang, X.; Wei-Chung Chang, V.; Li, Z.; Song, Y.; Li, C.; Wang, Y. Co-pyrolysis of sewage sludge and food waste digestate to synergistically improve biochar characteristics and heavy metals immobilization. *Waste Manag.* **2022**, *141*, 231–239. [CrossRef]
20. Wang, X.; Chang, V.W.-C.; Li, Z.; Chen, Z.; Wang, Y. Co-pyrolysis of sewage sludge and organic fractions of municipal solid waste: Synergistic effects on biochar properties and the environmental risk of heavy metals. *J. Hazard. Mater.* **2021**, *412*, 125200. [CrossRef]
21. Cui, Z.; Xu, G.; Ormeci, B.; Liu, H.; Zhang, Z. Transformation and stabilization of heavy metals during pyrolysis of organic and inorganic-dominated sewage sludges and their mechanisms. *Waste Manag.* **2022**, *150*, 57–65. [CrossRef] [PubMed]
22. Huang, C.; Wang, W.; Sun, X.; Shen, J.; Wang, L. A novel acetogenic bacteria isolated from waste activated sludge and its potential application for enhancing anaerobic digestion performance. *J. Environ. Manag.* **2020**, *255*, 109842. [CrossRef]
23. Zhang, P.; Zhang, X.; Li, Y.; Han, L. Influence of pyrolysis temperature on chemical speciation, leaching ability, and environmental risk of heavy metals in biochar derived from cow manure. *Bioresour. Technol.* **2020**, *302*, 1228500. [CrossRef]
24. Gu, W.; Guo, J.; Bai, J.; Dong, B.; Hu, J.; Zhuang, X.; Zhang, C.; Shih, K. Co-pyrolysis of sewage sludge and Ca(H2PO4)2: Heavy metal stabilization, mechanism, and toxic leaching. *J. Environ. Manag.* **2022**, *305*, 114292. [CrossRef]
25. Qi, Q.; Hu, C.; Lin, J.; Wang, X.; Tang, C.; Dai, Z.; Xu, J. Contamination with multiple heavy metals decreases microbial diver-sity and favors generalists as the keystones in microbial occurrence networks. *Environ. Pollut.* **2022**, *306*, 119406. [CrossRef]
26. Fan, Z.; Zhou, X.; Peng, Z.; Wan, S.; Gao, Z.F.; Deng, S.; Tong, L.; Han, W.; Chen, X. Co-pyrolysis technology for enhancing the functionality of sewage sludge biochar and immobilizing heavy metals. *Chemosphere* **2023**, *317*, 137929. [CrossRef]
27. Chen, J.; Liu, J.; He, Y.; Huang, L.; Sun, S.; Sun, J.; Chang, K.; Kuo, J.; Huang, S.; Ning, X. Investigation of co-combustion characteristics of sewage sludge and coffee grounds mixtures using thermogravimetric analysis coupled to artificial neural net-works modeling. *Bioresour. Technol.* **2017**, *225*, 234–245. [CrossRef]
28. Shen, X.; Zeng, J.; Zhang, D.; Wang, F.; Li, Y.; Yi, W. Effect of pyrolysis temperature on characteristics, chemical speciation and environmental risk of Cr, Mn, Cu, and Zn in biochars derived from pig manure. *Sci. Total Environ.* **2020**, *704*, 135283. [CrossRef]
29. Zhang, X.; Zhao, B.; Liu, H.; Zhao, Y.; Li, L. Effects of pyrolysis temperature on biochar's characteristics and speciation and environmental risks of heavy metals in sewage sludge biochars. *Environ. Technol. Inno.* **2022**, *26*, 102288. [CrossRef]
30. Liu, Z.; Liu, H.; Zhang, Y.; Lichtfouse, E. Efficient phosphate recycling by adsorption on alkaline sludge biochar. *Environ. Chem. Lett.* **2023**, *21*, 21–30. [CrossRef]
31. Zhang, S.; Gu, W.; Geng, Z.; Bai, J.; Dong, B.; Zhao, J.; Zhuang, X.; Shih, K. Immobilization of heavy metals in biochar by co-pyrolysis of sludge and $CaSiO_3$. *J. Environ. Manag.* **2023**, *326*, 116635. [CrossRef] [PubMed]
32. Xiaorui, L.; Longji, Y.; Xudong, Y. Evolution of chemical functional groups during torrefaction of rice straw. *Bioresour. Technol.* **2021**, *320*, 124328. [CrossRef] [PubMed]
33. Chen, X.; Ma, R.; Luo, J.; Huang, W.; Fang, L.; Sun, S.; Lin, J. Co-microwave pyrolysis of electroplating sludge and municipal sewage sludge to synergistically improve the immobilization of high-concentration heavy metals and an analysis of the mechanism. *J. Hazard. Mater.* **2021**, *417*, 126099. [CrossRef]
34. Tang, F.; Yu, H.; Yassin Hussain Abdalkarim, S.; Sun, J.; Fan, X.; Li, Y.; Zhou, Y.; Chiu Tam, K. Green acid-free hydrolysis of wasted pomelo peel to produce carboxylated cellulose nanofibers with super absorption/flocculation ability for environmental remediation materials. *Chem. Eng. J.* **2020**, *395*, 125070. [CrossRef]
35. Fang, S.; Yu, Z.; Lin, Y.; Hu, S.; Liao, Y.; Ma, X. Thermogravimetric analysis of the co-pyrolysis of paper sludge and municipal solid waste. *Energ. Convers. Manag.* **2015**, *101*, 626–631. [CrossRef]
36. Yang, Y.-Q.; Cui, M.-H.; Guo, J.-C.; Du, J.-J.; Zheng, Z.-Y.; Liu, H. Effects of co-pyrolysis of rice husk and sewage sludge on the bioavailability and environmental risks of Pb and Cd. *Environ. Technol.* **2021**, *42*, 2304–2312. [CrossRef]

37. Huang, H.; Yao, W.; Li, R.; Ali, A.; Du, J.; Guo, D.; Xiao, R.; Guo, Z.; Zhang, Z.; Awasthi, M.K. Effect of pyrolysis temperature on chemical form, behavior and environmental risk of Zn, Pb and Cd in biochar produced from phytoremediation residue. *Bioresour. Technol.* **2018**, *249*, 487–493. [CrossRef]
38. Chen, G.; Tian, S.; Liu, B.; Hu, M.; Ma, W.; Li, X. Stabilization of heavy metals during co-pyrolysis of sewage sludge and ex-cavated waste. *Waste Manag.* **2020**, *103*, 268–275. [CrossRef]
39. Xu, Y.; Qi, F.; Bai, T.; Yan, Y.; Wu, C.; An, Z.; Luo, S.; Huang, Z.; Xie, P. A further inquiry into co-pyrolysis of straws with manures for heavy metal immobilization in manure-derived biochars. *J. Hazard. Mater.* **2019**, *380*, 120870. [CrossRef]
40. Wang, Z.; Xie, L.; Liu, K.; Wang, J.; Zhu, H.; Song, Q.; Shu, X. Co-pyrolysis of sewage sludge and cotton stalks. *Waste Manag.* **2019**, *89*, 430–438. [CrossRef] [PubMed]
41. Li, Z.; Huang, Y.; Zhu, Z.; Yu, M.; Cheng, H.; Shi, H.; Zuo, W.; Zhou, H.; Wang, S. Co-pyrolysis of industrial sludge with phytoremediation residue: Improving immobilization of heavy metals at high temperature. *Fuel* **2023**, *351*, 128942. [CrossRef]

Disclaimer/Publisher's Note: The statements, opinions and data contained in all publications are solely those of the individual author(s) and contributor(s) and not of MDPI and/or the editor(s). MDPI and/or the editor(s) disclaim responsibility for any injury to people or property resulting from any ideas, methods, instructions or products referred to in the content.